5240 J. Med. Chem. 2010, 53, 5240–5247
DOI: 10.1021/jm100378b

Journal of Medicinal Chemistry Article

Oncocin (VDKPPYLPRPRPPRRIYNR-NH_2): A Novel Antibacterial Peptide Optimized against Gram-Negative Human Pathogens

Daniel Knappe,[†] Stefania Piantavigna,[‡] Anne Hansen,[†] Adam Mechler,[‡,∥] Annegret Binas,[§] Oliver Nolte,[§] Lisandra L. Martin,[‡] and Ralf Hoffmann*,[†]

[†]*Institute of Bioanalytical Chemistry, Universität Leipzig, Deutscher Platz 5, D-04103 Leipzig, Germany,* [‡]*School of Chemistry, Monash University, Clayton, 3800, Victoria, Australia, and* [§]*AiCuris GmbH & Co. KG, Friedrich-Ebert-Strasse 475, Building 302, D-42117 Wuppertal, Germany.* [∥]*Current address: School of Molecular Sciences, La Trobe University, Bundoora, Australia.*

Received March 26, 2010

Small proline-rich antimicrobial peptides (AMP) have attracted considerable interest, as they target specific intracellular bacterial components and do not act by lytic mechanisms. Here, a novel peptide, termed oncocin (VDKPPYLPRPRPPRRIYNR-NH_2), is reported that was optimized for the treatment of Gram-negative pathogens. Its minimal inhibitory concentrations in tryptic soy broth medium ranged from 0.125 to 8 μg/mL for 34 different strains and clinical isolates of Enterobacteriaceae and nonfermenters, such as *Escherichia coli*, *Pseudomonas aeruginosa*, and *Acinetobacter baumannii*. Substitutions of two arginine residues by ornithine increased the half-lives in full mouse serum from about 20 min to greater than 180 min and the activity. Both optimized oncocin derivatives were neither toxic to human cell lines nor hemolytic to human erythrocytes. They could freely penetrate lipid membranes and were washed out completely without any sign of lytic activity, as assessed by quartz crystal microbalance. Fluorescence labeled peptides entered the periplasmic space within 20 min at room temperature and homogeneously stained *E. coli* within 50 min. In conclusion, the optimized oncocin represents a very promising candidate for future in vivo work and may serve as a novel lead compound for an antibacterial drug class.

Introduction

The incidence of serious bacterial infections is increasing, especially for pathogens resistant to traditional antibiotics. In Europe an estimated three million hospitalized patients acquire nosocomial infections every year, accounting for approximately 50 000 deaths in the EU, as reported by the ECDC (European Centre for Disease Prevention and Control).[1] The U.S. Center for Disease Control and Prevention estimates 2 million nosocomial infections per year in the U.S., accounting for more than 50 000 deaths and more than U.S. $3.5 billion in additional health care costs. The Gram-positive pathogen methicillin resistant *Staphylococcus aureus*, (MRSA) attracts the most public interest. However, highly resistant Gram-negative pathogens are emerging, causing serious health care problems. Currently, three species of Enterobacteriaceae (*Escherichia coli*, *Klebsiella pneumoniae*, and *Enterobacter cloacae*) and two nonfermenting species (*Acinetobacter baumannii* and *Pseudomonas aeruginosa*) are causing much concern because of the rapid spread of multi or extremely resistant strains. This problem has developed initially from species in which single mutations were sufficient to cause clinically important resistance levels (*P. aeruginosa*) followed by bacteria with multiple mutations (*E. coli*). This has mainly been attributed to the broad prescription of fluoroquinolones.[2] Co-resistance to three antibiotic classes, including third-generation cephalosporins, has already become the fourth most common resistance pattern found for invasive *E. coli* in Europe. Important mechanisms of Gram-negative bacteria resistance include extended spectrum beta lactamases (ESBL) in *E. coli* or broad range beta lactamases like *K. pneumoniae* carbapenemase (KPC) in *K. pneumoniae*.[3−5] Multidrug resistant *A. baumannii*, associated with invasive infections such as pneumonia, meningitis, and bacteraemia, have been found to be responsible for outbreaks in hospitals especially in intensive care units.[6,7] Most frightening, pan-resistant *A. baumannii* clones were reported from outbreaks in the U.S. and were uniformly susceptible against only polymyxin treatment (e.g., colistin).[8]

Prudent use of existing antibiotics may slow down further resistance development. However, in order to provide effective treatment for the future, innovative antimicrobials are necessary, preferably with novel modes of action and/or belonging to novel drug classes.[9] More recently, inducible antimicrobial peptides (AMP[a]) have moved into the focus of

*To whom correspondence should be addressed. Phone: 49 (0) 341 9731330. Fax: 49 (0) 341 9731339. E-mail: Hoffmann@chemie.uni-leipzig.de.

[a]Abbreviations: ΔD, dissipation change; Δf, frequency change; AMP, antimicrobial peptides; ATCC, American Type Culture Collection; cfu, colony forming units; DIC, diisopropyl carbodiimide; DMPC, 1,2-dimyristoyl-*sn*-glycero-3-phosphocholine; DMPG, 1,2-dimyristoyl-*sn*-glycero-3-phosphoglycerol (sodium salt); DMSO, dimethyl sulfoxide; DSMZ, Deutsche Sammlung für Mikroorganismen und Zellkulturen; EDTA, ethylenediaminetetracetic acid; Fmoc, 9-fluorenylmethoxycarbonyl; HOBt, 1-hydroxybenzotriazole; ICB, Identification and Classification of Bacteria database; MIC, minimal inhibitory concentration; MPA, mercaptopropionic acid; ONPG, *o*-nitrophenyl-β-galactoside; PBS, phosphate buffered saline; QCM, quartz crystal microbalance; RP-HPLC, reversed-phase high performance liquid chromatography; SAM, self-assembled monolayer; SDS, sodium dodecyl sulfate; TAMRA, 5(6)-carboxytetramethylrhodamine; TSB, tryptic soy broth; TFA, trifluoroacetic acid; Tris-HCl, tris(hydroxymethyl)aminomethane hydrochloride; UTI, urinary tract infections.

 Published on Web 06/21/2010

Table 1. Sequences and MIC values of the *Oncopeltus* Antibacterial Peptide 4 and Its Analogues Derived by Substitutions in Positions 11, 19, and 20[a]

			monoisotopic mass, MIC (μg/mL)			
peptide	sequence	t_R [b] (min)	exptl[b]	calcd[b]	*E. coli* BL21 AI	*M. luteus* ATCC 10240
1	VDKPPYLPRP**P**PPRRIYNN**R-OH**	17.18	2445.41	2445.35	128	64
2	VDKPPYLPRP**T**PPRRIYNN**R-OH**	17.22	2449.38	2449.35	128	64
3	VDKPPYLPRP**H**PPRRIYNN**R-OH**	17.03	2485.41	2485.36	64	32
4	VDKPPYLPRP**K**PPRRIYNN**R-OH**	16.85	2476.44	2476.40	16	16
5	VDKPPYLPRP**R**PPRRIYNN**R-OH**	17.01	2504.43	2504.40	8	16
6	VDKPPYLPRP**R**PPRRIYNN**R-NH$_2$**	16.93	2503.49	2503.42	8	8
7	VDKPPYLPRP**R**PPRRIYN**RN-OH**	17.01	2504.44	2504.40	8	16
8	VDKPPYLPRP**R**PPRRIYN**RN-NH$_2$**	16.96	2503.41	2503.42	16	128
9	VDKPPYLPRP**R**PPRRIYN **R-OH**	17.13	2390.42	2390.36	32	64
10	VDKPPYLPRP**R**PPRRIYN **R-NH$_2$**	17.05	2389.38	2389.38	4	8
11	VDKPPYLPRP**R**PPR**O**IYN **O-NH$_2$**	16.71	2305.36	2305.33	8	8
12	VDKPPYLPRP**R**PPRRIYN-OH	17.36	2234.29	2234.26	64	128
13	VDKPPYLPRP**R**PPR-OH	16.67	1687.95	1687.97	nd	nd

[a] The antibacterial activities were determined against nonpathogenic *E. coli* and *M. luteus* strains using a serial dilution of the peptides in 1% TSB. nd: not determined. [b] t_R denotes retention times of the purified peptides on RP-HPLC, and calcd and exptl denote the calculated and experimentally determined monoisotopic masses of the quasimolecular ion $[M + H]^+$ recorded by MALDI-MS.

antimicrobial research for a number of reasons. AMP, ranging in size from 12 to 100 amino acid residues, have been identified in plants, animals, and microbes.[10] A single species typically produces more than six different AMP, where each peptide often exhibits a different activity spectrum.[11] Most of these AMP act directly on the bacterial membrane via disruptive "lytic" or pore-forming "ionophoric" mechanisms. This is a major concern for systemic treatments due to the possible toxic effects on mammalian cellular membranes at higher concentrations, which reduce the therapeutic index and limit their clinical potential. Consequently, investigation of these peptide classes mostly considers topical applications. However, such toxic effects might be overcome where AMP specifically target bacterial proteins without cross-reactivity toward human proteins. In recent years, one class of AMP that has attracted much interest is the small, proline-rich peptide family commonly found in both mammals, including humans (cathelicidins), and insects. These are predominantly active against Gram-negative bacteria including life threatening human pathogens, such as, *E. coli*, *K. pneumoniae*, and *P. aeruginosa*. The insect-derived Pro-rich AMP, such as abaecin, apidaecin, drosocin, formaecin, lebocin, and pyrrhocoricin,[12−16] are typically 20−35 residues long and have a relatively high proportion of basic amino acid residues. Among these AMP, drosocin and pyrrhocoricin have attracted much interest because their favorable antibacterial activities and low toxicity toward mammalian cell lines. Most notably, analogues have been designed with improved in vivo activities and pharmaceutical properties by the Otvos laboratory.[17]

The 2 kDa *Oncopeltus* antibacterial peptide 4 was originally isolated from *Oncopeltus fasciatus* (milkweed bug) together with three other AMP following infection with *P. aeruginosa* and *Pseudomonas putida*.[18] The amino acid sequence VDKPPYLPRP(X/P)PPRRIYN(NR) was determined by Edman degradation, although position 11 was uncertain and positions 19 and 20 were also questioned by the authors. This peptide showed a 70% sequence identity to pyrrhocoricin isolated from *Pyrrhocoris apterus*[16] as well as a 70% identity to the N-terminal 13 residues of both metalnikowin 1[19] and PR-39 isolated from *Palomena prasina* and *Sus scrofa*,[20] respectively. Because of the high proportion of proline (30%) and a large number of cationic amino acids (25%), this peptide is included in the family of Pro-rich AMP.

In this study, we investigated the antibacterial properties of the original sequence reported for *Oncopeltus* antibacterial peptide 4, which to the best of our knowledge has not been studied previously. Initially, the synthetic peptide was completely inactive toward both *E. coli* and *Micrococcus luteus*, so substitutions of amino acids into the ambiguous positions 11, 19, and 20 in the original sequence were included. In addition, the shortened and mutated 19-mer sequence containing a C-terminal amide (termed oncocin, peptide **10** (VDKPPYLPRPRPPRRIYNR-NH_2)) was found to be active toward 37 different isolates of *E. coli*, *K. pneumoniae*, *P. aeruginosa*, *A. baumannii*, *E. cloacae*, and *Proteus vulgaris*. The minimal inhibitory concentrations (MIC) for these bacterial stains and clinical isolates ranged from 0.125 to 8 μg/mL when tested in TSB medium. Oncocin (peptide **10**) was also found to be relatively stable in serum, nontoxic to SH-SY5Y and HeLa cells, and nonhemolytic. Furthermore, the fluorescein-labeled oncocin peptide penetrated *E. coli* cells within 50 min. The mechanism for peptide penetration using artificial lipid layers was also investigated by quartz crystal microbalance (QCM), which indicated that oncocin can freely traverse these lipid membranes and clearly does not act by a membrane disrupting or lytic mechanism. Such peptide−membrane characteristics support activity via an intracellular target.

Results

Surprisingly, the synthetic peptide corresponding to the reported sequence for *Oncopeltus* antibacterial peptide 4 (**1**, VDKPPYLPRPPPPRRIYNNR) was only very slightly active against *E. coli* BL21 AI and *M. luteus* (Table 1). Because peptide **1** contained several uncertain positions, we decided to substitute some residues to improve the activity. First, several variants were constructed for position 11 and tested. Threonine was an obvious choice because of the high sequence homologies to drosocin and pyrrhocoricin in this region; however, the activity did not improve for peptide **2** (Table 1). Basic amino acid residues such as His, Lys, and Arg (peptides **3**−**5**) were explored because they are also found in this class of AMP, and these variants were observed to improve the MIC-values: 8 μg/mL for *E. coli* BL21 AI and 16 μg/mL for *M. luteus*. The most active of these analogues, i.e., peptide **5** containing Arg in position 11 (Table 1), was then further modified at the two C-terminal residues. The Asn-Arg variant, corresponding to residues 19 and 20 of oncopeltus 4 was constructed (peptide **9**, Table 1). As the C-termini are always difficult to identify by Edman-sequencing, Asn and Arg

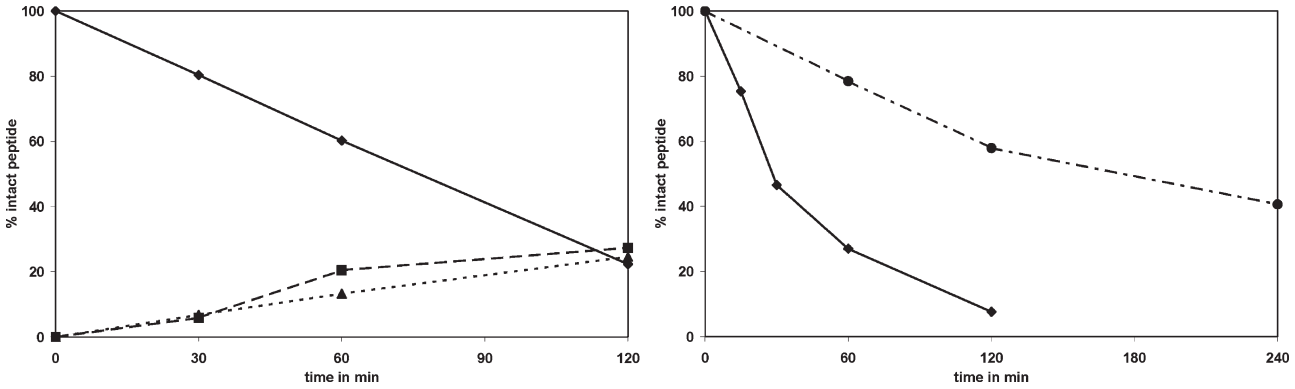

Figure 1. Stability of peptides **10** (solid line, both panels) and **11** (dots and dashes, right panel) in 25% aqueous (left) and undiluted mouse serum (right). The determined peptide amounts are shown relative to the peptide quantities obtained for an incubation time of 0 min (set to 100%). The two major degradation products identified by MALDI-MS corresponded to the N-terminal 18 residues (peptide **12**, dashed line, left panel) and 14 residues (peptide **13**, dotted line, left panel).

residues are typically detected as weak signals and were also questioned by Schneider's group.[18] Initially, these two residues were reversed (peptide **7**), as the resulting sequence would be homologous to the C-terminal last nine residues of the pyrrhocoricin sequence. However, the MIC values did not improve (Table 1). Then amidation of the C-termini of both peptides (peptides **6** and **8**) was explored; however, these did not influence the antibacterial activity. Interestingly, shortening the sequence by deletion of Asn19 reduced the activity by about 4-fold for the C-terminal acid analogue (peptide **9**), although the C-terminal amidation improved it by approximately 2-fold (peptide **10**). Finally the MIC values for the "optimized" peptide **10** were in good agreement with other related insect derived AMP. It is noted that the optimized sequence most likely does not represent the native peptide. Therefore, we use the term oncocin for the artificial sequence **10** (VDKPPYLPRPRPPRRIYNR-NH_2) indicating its relation to peptide **1**, i.e., the reported *Oncopeltus* antibacterial peptide 4.

The serum stability of peptide **10** (oncocin) was studied first in order to judge possible systemic pharmacological applications. Considering the unfolded, disordered peptide was only 19 residues, it was found to be relatively stable with a half-life of approximately 70 min in 25% aqueous serum at 37 °C (Figure 1, left). This compared well with peptide **9** with a free C-terminus with a half-life of less than 30 min (data not shown). Only two degradation products of peptide **10**, with cleavage sites C-terminal to Asn18 (peptide **12**) and Arg14 (peptide **13**), were detected after 30 min at the 10% level (Figure 1, left). The extent of degradation increased continuously to more than 20% of the original peptide after 2 h had elapsed. On the basis of the peak areas observed, these two metabolites and the remaining peptide **10** represented more than 60% of the original peptide content. This indicated that both metabolites were formed by two major degradation pathways and that both metabolites were more stable in serum than peptide **10** itself. The first metabolite, peptide **13**, probably results from a trypsin-like cleavage between the two Arg residues, whereas peptide **12** is more likely to be produced by the action of carboxypeptidases. The serum stabilities obtained are similar to other members of the family of short, proline-rich peptides reported recently.[21,22] Notably, as peptide **12** did not possess any antibacterial activity, it was deemed necessary to improve the stability of both cleavage sites. This was achieved by replacing Arg14 and Arg19 by ornithine (peptide **11**), an amino acid that is not attacked by trypsin and trypsin-like enzymes (Figure 1, right).[23] The half-life for the resulting peptide **11** in full serum was approximately 180 min compared to only about 20 min for peptide **10**. More importantly, no stable metabolite was detected for peptide **11**, indicating that the peptide is not degraded at a single site but more slowly at different positions. Peptide **11** also maintained the high antibacterial activities observed for the "optimized" peptide **10** (Table 1).

The third important criterion in which to judge the pharmacological properties of AMP in vitro is their toxicity against mammalian cell lines. Neither the optimized peptide **10** nor its double ornithine analogue (peptide **11**) showed any toxic effects on HeLa- or neuronal-cell-like differentiated SH-SY5Y cells (Figure 2, upper panel) at a peptide concentration of 600 μg/mL, which was about 100-fold above their MIC-values against *E. coli* BL21 AI. The observed nontoxicity was also found for two other insect derived peptides of this AMP family, i.e., drosocin and apidaecin 1b (Figure 2, upper panel). Moreover, none of the tested peptides showed any hemolytic activity against human erythrocytes in the studied peptide concentration range up to 600 μg/mL (Figure 2, lower panel).

Although the nonpathogenic bacterial strains *E. coli* BL21 AI and *M. luteus* were originally used to optimize the antibacterial properties of oncocin (peptide **10**), they do not allow the pharmacological properties of this lead compound to be assessed against human pathogens. Therefore, we tested a broad panel of 37 strains and clinical isolates from seven Gram-negative bacteria (Table 2). The MIC values for the eight *E. coli* strains tested and clinical isolates were very similar ranging from 0.5 to 8 μg/mL for peptide **10** and only 0.5 to 2 μg/mL for peptide **11**. Thus, the double ornithine analogue was equally active against all *E. coli* strains with an average MIC value of 1 μg/mL. Interestingly, both peptides showed equal activities against *E. coli* strains very prone to peptide **10** but were different for strains less prone to peptide **10**, such as *E. coli* 70419002. This improved activity of peptide **11** could be related to its higher protease resistance, as indicated by the serum stability. The peptide might be stable over longer times in the medium (or bacteria) and thus kill the bacteria more effectively. This effect was also observed for *P. aeruginosa* and *K. pneumoniae* (Table 2). The MIC values of peptide **11** varied only between 1 and 4 μg/mL among the eight *P. aeruginosa* strains and clinical isolates and between 0.5 and 2 μg/mL among the six *K. pneumoniae* strains and clinical

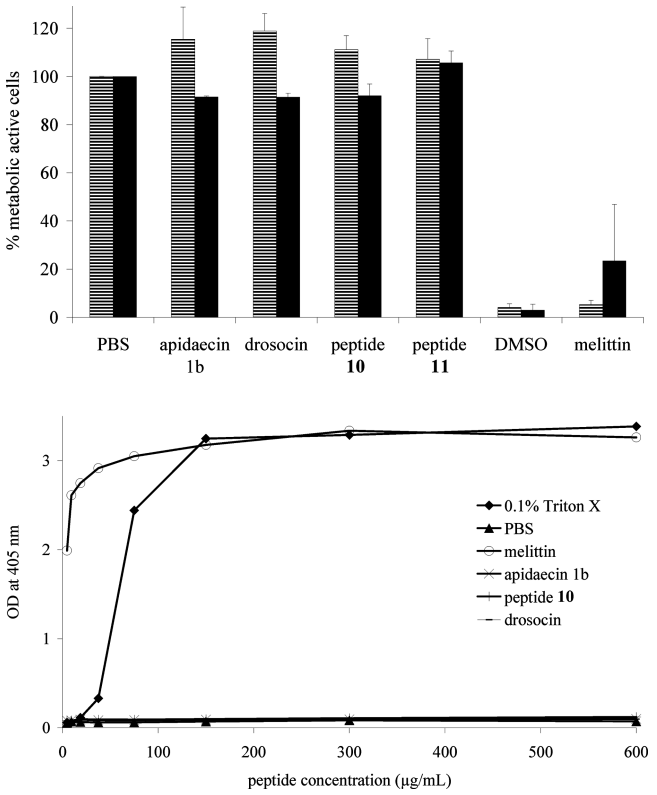

Figure 2. Cytotoxicity against HeLa cells (full bars) and differentiated SH-SY5Y cells (striped bars) using the MTT cell proliferation assay (upper panel) and hemolytic activity (lower panel) of different antimicrobial peptides. SH-SY5Y and HeLa cells were incubated with AMP (600 μg/mL), melittin (100 μg/mL), and DMSO (12% (v:v), positive control) for 24 h. The data were normalized to PBS (100%) as negative control. Human erythrocytes were incubated with a 2-fold serial dilution of a peptide (600 to 5 μg/mL), Triton X-100 (0.1%, positive control), and PBS (negative control) at 37 °C for 60 min.

isolates tested (Table 2). Thus, peptide **11** was in general more active against the tested Gram-negative human pathogens than oncocin with less variation among the bacterial strains and clinical isolates. Although in vitro data cannot be simply extrapolated to animal models, both peptides **10** and **11** represent new promising lead compounds with interesting antibacterial properties.

The interaction between peptides **10** and **11** with bacterial mimetic membranes was followed using a quartz crystal microbalance (QCM).[24] Supported lipid bilayers composed of DMPC−DMPG (4:1) were prepared on the gold coated quartz crystal, and the response of the frequency change (Δf) with time for a series of harmonic resonances was monitored as described in our earlier work.[24,25] The concentration dependence of the peptides binding to the membrane for 1−15 μM peptide **10** is shown in Figure 3A, and that for peptide **11** is shown in Figure 3B. The rapid incorporation of the peptides into the membrane is apparent by the initial slope of the $\Delta f-t$ traces prior to the saturation of the membrane at ~10 min. For both peptides the 1 μM solutions show subsaturation of the membrane, whereas 5−15 μM appears to saturate the membranes albeit with a slightly greater mass of the modified peptide **11** binding. To elucidate the nature of the peptide−membrane interaction, these data were recorded over multiple harmonics and both peptides showed responses consistent with transmembrane binding (data not shown).

Table 2. Broad Spectrum Antimicrobial Activity of Peptides **10** and **11** against Different Gram-Negative Pathogens (Reference [DSM, ATCC, IBC] and Clinical Isolates) Determined in 1% TSB

	MIC (μg/mL)	
pathogen	peptide **10**	peptide **11**
P. aeruginosa DSM3227	4	4
P. aeruginosa Walter	8	4
P. aeruginosa ATCC27853	4	2
P. aeruginosa PAO1	2	2
P. aeruginosa 60811001	2	2
P. aeruginosa 60909001	2	1
P. aeruginosa 61118003	2	1
P. aeruginosa 70108001	4	2
E. coli 70329001	1	1
E. coli 70430001	1	0.5
E. coli 70419002	8	2
E. coli 70502001	1	1
E. coli Neumann	2	0.5
E. coli 205024	4	1
E. coli 455/7	0.5	0.5
E. coli 8474	0.5	0.5
K. pneumoniae DSM681	0.25	0.5
K. pneumoniae 57 USA	0.25	0.5
K. pneumoniae 63	8	2
K. pneumoniae 8085	0.5	0.5
K. pneumoniae ATCC12657	0.5	0.5
K. pneumoniae ATCC27799	1	1
A. baumannii ICB14067	1	1
A. baumannii ICB14072	1	1
A. baumannii ICB14073	2	1
A. baumannii ICB9250	0.5	0.5
A. baumannii M17	1	1
E. cloacae 34654	0.25	0.5
E. cloacae Ha088	0.125	0.25
E. cloacae Ha089	0.125	0.25
E. cloacae Ha185	0.5	0.5
E. cloacae Ha89	0.25	0.25
P. vulgaris ICB9081	4	8
P. vulgaris ICB9095	4	4
Stenotrophomonas ICB308054	32	32
Stenotrophomonas ICB7569	8	16
Stenotrophomonas ICB7789	32	32

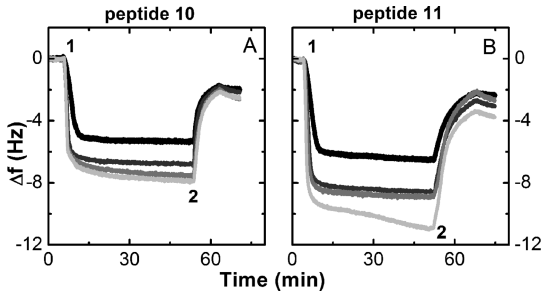

Figure 3. Peptides **10** (A) and **11** (B) uptake on DMPC−DMPG (4:1) membrane as a function of peptide concentration (1, 5, 10, 15 μM peptide corresponds to darkest to lightest color). The number "1" indicates the points where the peptide solution was introduced. Only the seventh harmonic data are shown. Data have been normalized to zero for the membrane coated chip in high salt buffer. The number "2" indicates introduction of buffer wash at 100 μL min^{-1}.

Interestingly, the peptide−membrane interactions for both peptides **10** and **11** were not permanent, as the introduction of the PBS solution (position 2 in Figure 3) resulted in removal of almost the entire mass of bound peptide. In both cases, a residual amount of peptide remained in the membrane, between ~2 Hz for peptide **10** and ~3 Hz for peptide **11**.

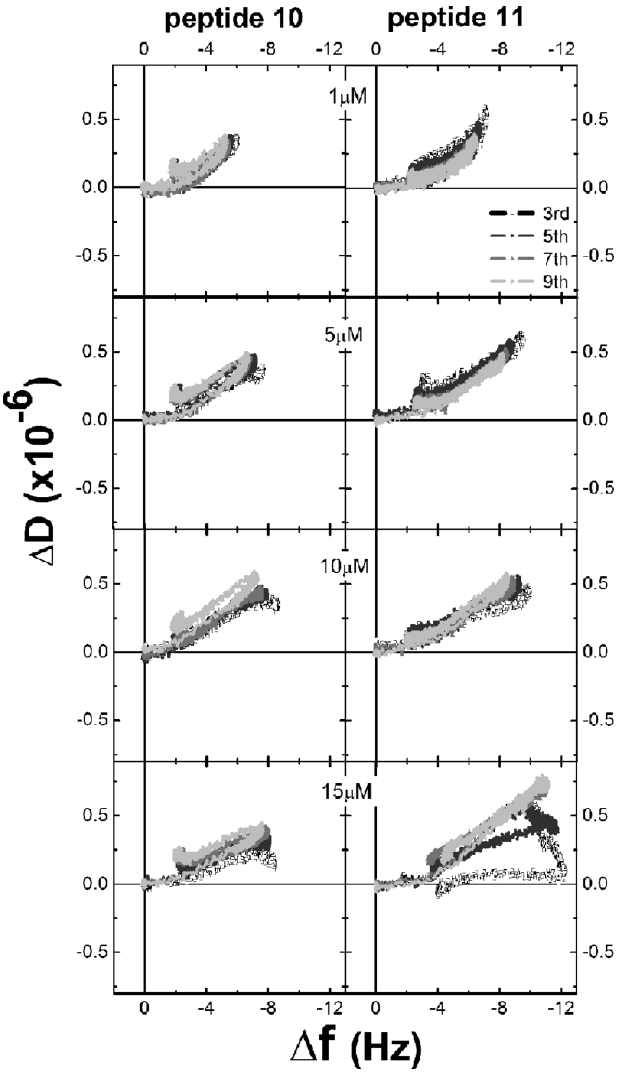

Figure 4. Energy dissipation (ΔD) vs frequency (Δf) dependence for peptides **10** (left column) and **11** (right column) on DMPC−DMPG (4:1) membrane bilayer. The peptide concentrations increase from 1 to 15 μM (top to bottom), and data from the third, fifth, seventh, and ninth harmonic are shown.

The QCM data can also contribute to our understanding of the mechanism of each peptide interacting with the membrane. The characteristic *fingerprint* for each peptide interaction is recorded as the change in energy dissipation, ΔD [25,26] measured simultaneously with the temporal variation in the frequency, Δf. Thus, the dependence of ΔD versus Δf provides an assessment of the structural influence of the peptide binding per unit mass (i.e., $-\Delta f$) on the membrane properties.[25−27] Figure 4 shows the $\Delta D-\Delta f$ plots for peptides **10** (left column) and **11** (right column) for 1, 5, 10, and 15 μM (top to bottom panels). For each of these plots, the addition of the peptide solution (point 1 on Figure 3) has been set to the origin. Both peptide *fingerprints* show a similar trend, with the uptake of the peptide (more negative frequency) having a minimal effect on the membrane properties (only a small increase in dissipation). Notably, the change of the dissipation was very similar for the two peptides and over all the concentrations. This supports the same mechanism of peptide interaction with the membrane which is also independent of concentration. Furthermore, these plots confirm that the peptide uptake was reversible because the wash with PBS solution, which corresponds to the furthest point (maximum $-\Delta f$ and corresponding to point 2 in Figure 3), shows the dissipation returning to the origin, indicating that most of the peptide was removed from the membrane layer. Nevertheless, the buffer was unable to remove all the peptide, leaving some mass (presumably peptide molecules) associated with the membrane regardless of the concentration (~ 2 Hz for peptide **10** and ~3 Hz for peptide **11**). The $\Delta D-\Delta f$ plots also confirmed that for both peptides all four harmonics probed in these experiments responded similarly, supporting transmembrane peptide insertion across the lipid bilayer without causing a substantial perturbation to the membrane.

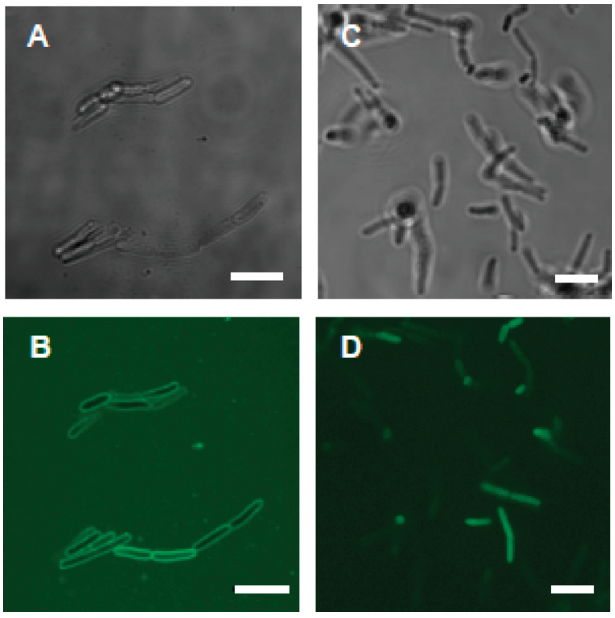

Figure 5. Confocal laser scanning microscopy images of *E. coli* BL21 AI cultures incubated with 5(6)-carboxyfluorescein-labeled peptide **10** (30 μmol/L) for 20 min (A, B) or 50 min (C, D). The fluorescence of the medium was quenched with TAMRA (180 μM). Shown are the phase contrast (A, C) and fluorescence images (B, D). Bars equate to 5 μm.

On the basis of the QCM studies with artificial membranes and following the hypothesis that small, proline-rich peptides kill bacteria by entering the cells and inhibiting intracellular targets like DnaK,[28] peptide **10** N-terminally labeled with 5(6)-carboxyfluorescein was added to an *E. coli* BL21 AI culture. Confocal fluorescence microscopy revealed that the fluorescence is first enriched at or close to the surface of *E. coli* cells after 20 min at room temperature before it is homogenously distributed within the living bacterial cells (Figure 5). This clearly indicates that peptide **10** penetrates the bacterial membrane relatively quickly and stays either in the membrane or in the periplasmic space before it is most likely actively transported into the cells. Similar observations were also reported for apidaecin,[29,30] pyrrhocoricin,[28] and Bac7.[31]

Discussion

Currently, most infections can be treated with available antibiotics, even if in some cases combination therapies might by mandatory. While a couple of new antimicrobials are in the pipeline or have already been launched for the treatment of MRSA and other Gram-positive pathogens, there is a lack of promising candidates active against Gram-negative pathogens. Importantly, Gram-negative bacteria are far more effective in

accumulating resistance traits; thus, new antimicrobials *are* needed.[32] In the current paper we reported the optimization of the naturally occurring *Oncopeltus* peptide 4 (peptide **1**) to the "optimized" peptide **11**, exhibiting promising antibacterial activity against the most serious Gram-negative pathogens. Starting with peptide **1**, which to the best of our knowledge has not been investigated for its antimicrobial properties, it was possible to obtain high antibacterial activity against *E. coli* by substituting position 11 against arginine and deleting asparagine at position 19. The activity of the 19-residue-long peptide **9** was further enhanced by C-terminal amidation. The limited protease resistance of peptide **10** was identified as a major weakness for therapeutic peptide applications and was overcome by substituting arginine by ornithine residues at positions 15 and 19. Despite ornithine not occurring naturally in proteins, the modified peptide **11** did not show any toxic effects against HeLa- and differentiated SH-SY5Y-cell cultures or hemolytic effects against erythrocytes. Considering the blood volume of animals and humans relative to their body weight, the tested peptide concentration of 600 μg/mL corresponds to a peptide dose of more than 60 mg/kg administered intravenously (i.v.). Although in vitro data have to be interpreted with caution, the lack of toxicity against mammalian cells together with the high activity against Gram-negative bacteria can be explained by their mode of action. Data published for apidaecin, pyrrhocoricin, and drosocin[28,30,31] clearly indicate that this class of insect-derived short, proline-rich peptides does not act by a lytic mechanism but kills the bacteria by inhibiting intracellular targets, such as DnaK.[33−35] This rapid intracellular incorporation was supported by the QCM data for peptides **10** and **11**, as they showed no tendency to disrupt or remove any lipids from the bilayer within the concentration range studied. Instead both peptides entered and left the DMPC−DMPG (4:1) lipid bilayers freely and relatively quickly, although the process was not completely quantitative following the PBS wash step. This small amount of residual peptide binding, however, is most likely attributed to some nonspecific binding to the interface between the underlying negatively charged surface of the modified QCM crystal and lipid bilayer. The nonlytic mechanism was further supported by fluorescence microscopy by incubating *E. coli* with 5(6)-carboxyfluorescein-labeled oncocin. The bacterial cells were not lysed during the observation interval of 1 h. Instead the outer layer of the cells was stained indicating a fast penetration of the peptide through the bacterial membrane (Figure 5). Any peptides bound onto the outer surface of the membrane would have been quenched by TAMRA added in high concentrations to the bacterial culture. Likely, the peptides penetrated through the bacterial membrane into the periplasmic space, where they accumulated within 20 min. With the separation in the periplasmic space from TAMRA added to the surrounding medium, the fluorescence was not quenched anymore. From there the peptides entered into the cells in a second step resulting in a homogeneous fluorescence staining throughout the bacterial cell, as much as this can be judged from the limited resolution of confocal microscopy. Once inside the cell the peptides probably inhibited one or more target proteins, such as DnaK,[33−35] and thereby killed the cells slowly without membrane lysis. Although many steps of the peptide uptake and the inhibition of the bacterial targets remain unclear, the slowly emerging underlying mechanisms explain nicely the high specificity of oncocin toward Gram-negative bacteria together with their very low intrinsic toxicity. For all these reasons the optimized oncocin sequences represent scientifically interesting and therapeutically promising new antibacterial candidates. Although confirmation with a larger collection of isolates is required, their antibacterial spectrum covers perfectly the currently most relevant Gram-negative human pathogens. While these continue to notoriously acquire resistance traits, our novel peptide will most likely not be affected by cross-resistance due to its novel mode of action.

Three bacteria, *E. coli*, *Klebsiella* species, and *Enterobacter* species account for 80−90% of uncomplicated urinary tract infections (UTI).[36] Thus, oncocin may provide complete coverage in this indication, and further research on oncocin should focus first on UTI animal models. The high serum stability obtained for peptide **11** and the ability to also kill nonfermenters (i.e., *A. baumannii* and *P. aeruginosa*) also suggest that severe systemic infections (i.e., pneumonia, bacteraemia, septicemia) could also be treated. Such in vivo and further in vitro studies have been initiated, and these will be published at a later time.

Conclusion

Using a combination of in vitro assays to study the (i) antibacterial activity against Gram-negative human pathogens, (ii) peptide stability against serum proteases, (iii) hemolytic activity against human erythocytes, (iv) cytotoxicity, and (v) interaction with artificial lipid bilayers, we could chemically optimize a 19-residue-long sequence called oncocin for systemic treatments. Oncocin (peptide **10**) and its even more promising analogue peptide **11** contain only natural α L-amino acids and were both synthesized on solid phase in high yields and purities. Thus, oncocin and its analogues represent a promising new class of peptide candidates to treat UTI and systemic infections, based on their superior biomedical properties together with the nonlytic mode of action targeting intracellular bacterial proteins.

Experimental Section

Peptide Synthesis. Peptides were synthesized on Rink amide MBHA resin or Wang resin (MultiSynTech GmbH, Witten, Germany) with standard 9-fluorenylmethoxycarbonyl/*tert*-butyl (Fmoc/^{t}Bu) chemistry using a 25 μmol scale on the multiple synthesizer SYRO2000 (MultiSynTech). Amino acid derivatives (> 99%, Orpegen Pharma, Heidelberg, Germany) were activated in situ with diisopropyl carbodiimide (DIC, > 98% by GC, Fluka Chemie GmbH; Buchs, Switzerland) in the presence of 1-hydroxybenzotriazole (HOBt, > 98%, Fluka Chemie).[37] After completion of the peptide synthesis, 5(6)-carboxyfluorescein (Fluka Chemie GmbH) was coupled to the unprotected N-terminus with DIC/HOBT using a part of the resin. The unlabeled or fluorescein-labeled peptides were cleaved with trifluoroacetic acid (TFA, > 98%) containing 12.5% (v:v) of a scavenger mixture (ethandithiole, *m*-cresole, thioanisole, and water, 2.5:5:5:5). The peptides were precipitated with cold diethyl ether and purified by RP-HPLC using a linear aqueous acetonitrile gradient in the presence of an ion pair reagent (eluent A, 0.1% aqueous TFA (> 99%); eluent B, 60% aqueous acetonitrile (> 99.95% by GC) containing 0.1% TFA) and a Jupiter C_{18} column (21.2 mm internal diameter, 250 mm length, 15 μm particle size, 30 nm pore size) (Phenomenex Inc., Torrance, CA). The purified peptides were analyzed by RP-HPLC on a Jupiter C_{18} column (4.6 mm internal diameter, 150 mm length, 5 μm particle size, 30 nm pore size; Phenomenex) using a linear gradient from 5% to 56% eluent B for 17 min (see Supporting Information). The purities were above 95% based on the peak areas obtained after background correction. The molecular weight of the peptide was confirmed by

matrix-assisted laser desorption/ionization time-of-flight mass spectrometry (MALDI-TOF-MS; 4700 proteomic analyzer; Applied Biosystems GmbH, Darmstadt, Germany) using α-cyano-4-hydroxycinnamic acid (4 mg/mL in 60% aqueous acetonitrile containing 0.1% TFA) as matrix (see Supporting Information).

Bacterial Strains. Nonpathogenic strains *E. coli* BL21AI and *M. luteus* ATCC 10240 were cultured overnight at 37 °C in nutrient broth (Carl Roth GmbH, Karlsruhe, Germany). All other (pathogenic) bacteria strains were cultured on solid Columbia agar. After overnight culture, colonies were suspended in sterile 0.9% saline to an OD of 0.1. This solution was diluted 1:300 in 1% TSB broth. An amount of 90 μL of the diluted bacteria was used for the microdilution assays per well.

Antibacterial Activity. The MIC values were determined in triplicate by a liquid broth microdilution assay in sterile 96-well plates (Greiner Bio-One GmbH, Frickenhausen, Germany) using a total volume of 100 μL per well.[38] Aqueous peptide solutions (1 mg/mL) were serially 2-fold diluted in 1% TSB starting at 128 μg/mL down to typically 0.5 μg/mL in eight steps. Overnight cultures of nonpathogenic bacteria were diluted with 1% TSB to 1.5×10^7 cells/mL (*E. coli* BL21AI) or 4×10^7 cells/mL (*M. luteus* ATCC 10240) and an amount of 50 μL was added to each well, gaining a starting cell concentration of 7.5×10^5 cells/well and 2×10^6 cells/well, respectively. An amount of 90 μL of the diluted suspension of the other pathogenic bacteria was used per well, giving a final cfu count (colony forming units) of $(1-2) \times 10^5$ cells/well. The plates were incubated at 37 °C, and the absorbance of each well was measured after 20 ± 2 h at 595 nm. The MIC was defined as the lowest peptide concentration where the absorbance value did not exceed that of the medium only.

Serum Stability Assays. The serum stabilities of all peptides were determined in pure and 25% (v:v) aqueous pooled mouse serum (PAA Laboratories GmbH, Pasching, Austria).[39] Peptides were dissolved in serum at a final concentration of 75 μg/mL and incubated at 37 °C. Aliquots taken in triplicate after 0, 30, 60, 120, and 240 min were precipitated by addition of trichloroacetic acid to a final concentration of 3% (v:v). After 10 min on ice, the samples were centrifuged and the supernatant was neutralized with sodium hydroxide solution (1 mol/L) and stored at −20 °C. The samples were analyzed on the analytical Jupiter C_{18} column using a linear aqueous acetonitrile or methanol gradient containing 0.1% (v:v) TFA. The metabolites were identified by MALDI-TOF-MS.

Quartz Crystal Microbalance (QCM). The mechanism in which these peptides bind to artificial membranes was studied in real time using a QCM-D instrument (Q-sense, Sweden), and the experimental design and methodology are based on published procedures.[24] Liposomes were prepared and deposited onto the gold chip and washed with buffer using "high salt" PBS buffer (0.02 M potassium phosphate, 0.1 M NaCl, pH 6.9).[25] A second "low salt" (0.01 M potassium phosphate, 0.03 M NaCl, pH 6.9) wash step was included to remove unopened liposomes prior to the return to a "high salt" PBS buffer medium. The peptide solution was then introduced, and the change in frequency (Δf) and dissipation (ΔD) was recorded for the third, fifth, seventh, and ninth harmonics over approximately 60 min for each experiment.

Confocal Laser Scanning Fluorescence Microscopy. An overnight culture of bacteria was diluted to 1.5×10^7 cells/mL in 1% TSB. A 5(6)-carboxyfluorescein-labeled peptide was added to the suspension together with a 60-fold molar excess of 5(6)-carboxytetramethylrhodamine (TAMRA; Merck, Darmstadt, Germany) to obtain a final peptide concentration of 30 μmol/L. Aliquots of the suspension (2 μL) were spotted on the microscope slides and immediately analyzed on an inverted confocal laser scanning microscope TCS SP5 (argon laser line 488 nm; objective, HCX PL APO lambda blue 63.0×1.40 Oil UV; software Leica Application Suite Advanced Fluorescence 1.7.2; Adobe Photoshop CS) (Leica Microsystems, Wetzlar, Germany).

Hemolytic Activity.[40] Peptides were serially diluted from 600 to 5 μg/mL in phosphate buffered saline (PBS, 8.7 mmol/L Na_2HPO_4, 1.2 mmol/L KH_2PO_4, 150 mmol/L NaCl, pH 7.4) in a V-bottom 96-well polypropylene plate (Greiner Bio-One GmbH) to a final volume of 100 μL. Concentrated human erythrocytes were washed and suspended in PBS to a final concentration of 2%. Aliquots of this suspension (100 μL) were added to the peptide solution in each well and incubated (37 °C, 1 h). After centrifugation (1000*g*), the absorbance of the supernatants was determined in a fresh F-bottom 96-well plate at 405 nm in a Sunrise microplate reader. The positive and negative controls contained 0.1% Triton X-100 and PBS, respectively, added at the same volumes as the peptide solution.

Cytotoxicity Assay. Cells were cultured in DMEM/Ham's F-12 medium with 15% (SH-SY5Y) or 5% (HeLa) (v:v) fetal bovine serum containing 1% (w:v) nonessential amino acids and 1% (w:v) streptomycin/penicillin at 37 °C and 5% CO_2. SH-SY5Y (2×10^4 cells per well) and HeLa cells (1.5×10^4 per well) were seeded in the same medium into 96-well plates (Greiner Bio-One GmbH). After 1 night (HeLa) or after 5 days of differentiation by 10 μM *trans*-retinoic acid (SH-SY5Y), cells were washed with PBS and fresh medium was added. Subsequently, the peptide solutions (100 μL per well, 600 μg/mL) were added and incubated again at identical conditions for 24 h. The cell viability was determined with the cell proliferation kit I (Roche Diagnostics GmbH; Mannheim, Germany). Briefly, an amount of 10 μL of the methylthiazolyldiphenyltetrazolium bromide (MTT) reagent was added to a final concentration of 0.5 mg/mL. After incubation (4 h, 37 °C, 5% CO_2) a sodium dodecyl sulfate (SDS) solution (10% (w:v) in 10 mmol/L hydrochloric acid, 100 μL) was added and incubated again at the same conditions (16 h). The absorbance at 590 nm was measured using a Paradigm microplate reader (Beckman Coulter, Wals, Austria) relative to a reference wavelength of 650 nm. The increased absorbance was used to estimate the viability of the cells. In the positive and negative controls the peptide solution was substituted by the same volumes of dimethyl sulfoxide (DMSO) and PBS, respectively.

Acknowledgment. We thank Prof. Peter Seibel and Mr. Ingo Schäfer for recording the confocal microscope images. Financial supports from the European Fund for Regional Structure Development (EFRE, European Union and Free State Saxony) and the BMBF (Innoprofile) are gratefully acknowledged. L.L.M. and A.M. thank the Australian Research Council for financial support through the Discovery Grant DP0662816.

Supporting Information Available: Reversed phase HPLC chromatograms and MALDI mass spectra for peptides **1**−**12**, as summarized in Table 1. This material is available free of charge via the Internet at http://pubs.acs.org.

References

(1) Amato-Gauci, A.; Ammon, A. *The First European Communicable Disease Epidemiological Report*; European Centre for Disease Prevention and Control: Stockholm, Sweden, 2007.
(2) Hooper, D. C. Emerging mechanisms of fluoroquinolone resistance. *Emerging Infect. Dis.* **2001**, *7*, 337–341.
(3) Jones, R. N. Resistance patterns among nosocomial pathogens. Trends over the past few years. *Chest* **2001**, *119*, 397S–404S.
(4) Pitout, J. D. D.; Laupland, K. B. Extended-spectrum beta-lactamase-producing enterobacteriaceae: an emerging public-health concern. *Lancet Infect. Dis.* **2008**, *8*, 159–166.
(5) Bradford, P. A.; Bratu, S.; Urban, C.; Visalli, M.; Mariano, N.; Landman, D.; Rahal, J. J.; Brooks, S.; Cebular, S.; Quale, J. Emergence of carbapenem-resistant Klebsiella species possessing the class A carbapenem-hydrolyzing KPC-2 and inhibitor-resistant TEM-30 beta-lactamases in New York City. *Clin. Infect. Dis.* **2004**, *39*, 55–60.

(6) Fournier, P. E.; Richet, H. The epidemiology and control of *Acinetobacter baumannii* in health care facilities. *Clin. Infect. Dis.* **2006**, *42*, 692–699.
(7) Katsaragakis, S.; Markogiannakis, H.; Toutouzas, K. G.; Drimousis, P.; Larentzakis, A.; Theodoraki, E. M.; Theodorou, D. *Acinetobacter baumannii* infections in a surgical intensive care unit: predictors of multi-drug resistance. *World J. Surg.* **2008**, *32*, 1194–1202.
(8) Lolans, K.; Rice, T. W.; Munoz-Price, L. S.; Quinn, J. P. Multicity outbreak of carbapenem-resistant *Acinetobacter baumannii* isolates producing the carbapenemase OXA-40. *Antimicrob. Agents Chemother.* **2006**, *50*, 2941–2945.
(9) Boucher, H. W.; Talbot, G. H.; Bradley, J. S.; Edwards, J. E.; Gilbert, D.; Rice, L. B.; Scheld, M.; Spellberg, B.; Bartlett, J. Bad bugs, no drugs: no ESKAPE! An update from the Infectious Diseases Society of America. *Clin. Infect. Dis.* **2009**, *48*, 1–12.
(10) Boman, H. G. Peptide antibiotics and their role in innate immunity. *Annu. Rev. Immunol.* **1995**, *13*, 61–92.
(11) Barra, D.; Simmaco, M.; Boman, H. G. Gene-encoded peptide antibiotics and innate immunity. Do "animalcules" have defence budgets? *FEBS Lett.* **1998**, *430*, 130–134.
(12) Casteels, P.; Ampe, C.; Jacobs, F.; Vaeck, M.; Tempst, P. Apidaecins. Antibacterial peptides from honeybees. *EMBO J.* **1989**, *8*, 2387–2391.
(13) Bulet, P.; Dimarcq, J. L.; Hetru, C.; Lagueux, M.; Charlet, M.; Hegy, G.; Vandorsselaer, A.; Hoffmann, J. A. A novel inducible antibacterial peptide of *Drosophila* carries an O-glycosylated substitution. *J. Biol. Chem.* **1993**, *268*, 14893–14897.
(14) Mackintosh, J. A.; Veal, D. A.; Beattie, A. J.; Gooley, A. A. Isolation from an ant *Myrmecia gulosa* of two inducible O-glycosylated proline-rich antibacterial peptides. *J. Biol. Chem.* **1998**, *273*, 6139–6143.
(15) Hara, S.; Yamakawa, M. A novel antibacterial peptide family isolated from the silkworm, *Bombyx mori*. *Biochem. J.* **1995**, *310*, 651–656.
(16) Cociancich, S.; Dupont, A.; Hegy, G.; Lanot, R.; Holder, F.; Hetru, C.; Hoffmann, J. A.; Bulet, P. Novel inducible antibacterial peptides from a hemipteran insect, the sap-sucking bug *Pyrrhocoris apterus*. *Biochem. J.* **1994**, *300*, 567–575.
(17) Otvos, L.; Wade, J. D.; Lin, F.; Condie, B. A.; Hanrieder, J.; Hoffmann, R. Designer antibacterial peptides kill fluoroquinolone-resistant clinical isolates. *J. Med. Chem.* **2005**, *48*, 5349–5359.
(18) Schneider, M.; Dorn, A. Differential infectivity of two pseudomonas species and the immune response in the milkweed bug, *Oncopeltus fasciatus* (Insecta: Hemiptera). *J. Invertebr. Pathol.* **2001**, *78*, 135–140.
(19) Chernysh, S.; Cociancich, S.; Briand, J. P.; Hetru, C.; Bulet, P. The inducible antibacterial peptides of the hemipteran insect *Palomena prasina*: identification of a unique family of proline-rich peptides and of a novel insect defensin. *J. Insect Physiol.* **1996**, *42*, 81–89.
(20) Agerberth, B.; Lee, J. Y.; Bergman, T.; Carlquist, M.; Boman, H. G.; Mutt, V.; Jornvall, H. Amino-acid-sequence of Pr-39. Isolation from pig intestine of a new member of the family of proline-arginine-rich antibacterial peptides. *Eur. J. Biochem.* **1991**, *202*, 849–854.
(21) de Visser, P. C.; van Hooft, P. A. V.; de Vries, A. M.; de Jong, A.; van der Marel, G. A.; Overkleeft, H. S.; Noort, D. Biological evaluation of Tyr6 and Ser7 modified drosocin analogues. *Bioorg. Med. Chem. Lett.* **2005**, *15*, 2902–2905.
(22) Noto, P. B.; Abbadessa, G.; Cassone, M.; Mateo, G. D.; Agelan, A.; Wade, J. D.; Szabo, D.; Kocsis, B.; Nagy, K.; Rozgonyi, F.; Otvos, L. Alternative stabilities of a proline-rich antibacterial peptide in vitro and in vivo. *Protein Sci.* **2008**, *17*, 1249–1255.
(23) Witkowska, E.; Orlowska, A.; Sagan, B.; Smoluch, M.; Izdebski, J. Tryptic hydrolysis of hGH-RH(1−29)-NH2 analogues containing Lys or Orn in positions 12 and 21. *J. Pept. Sci.* **2001**, *7*, 166–172.
(24) Mechler, A.; Praporski, S.; Atmuri, K.; Boland, M.; Separovic, F.; Martin, L. L. Specific and selective peptide−membrane interactions revealed using quartz crystal microbalance. *Biophys. J.* **2007**, *93*, 3907–3916.
(25) Piantavigna, S.; Czihal, P.; Mechler, A.; Richter, M.; Hoffmann, R.; Martin, L. L. Cell penetrating apidaecin peptide interactions with biomimetic phospholipid membranes. *Int. J. Pept. Res. Ther.* **2009**, *15*, 139–146.
(26) Mechler, A.; Praporski, S.; Piantavigna, S.; Heaton, S. M.; Hall, K. N.; Aguilar, M. I.; Martin, L. L. Structure and homogeneity of pseudo-physiological phospholipid bilayers and their deposition characteristics on carboxylic acid terminated self-assembled monolayers. *Biomaterials* **2009**, *30*, 682–689.
(27) Sherman, P. J.; Jackway, R. J.; Gehman, J. D.; Praporski, S.; McCubbin, G. A.; Mechler, A.; Martin, L. L.; Separovic, F.; Bowie, J. H. Solution structure and membrane interactions of the antimicrobial peptide fallaxidin 4.1a: an NMR and QCM study. *Biochemistry* **2009**, *48*, 11892–11901.
(28) Kragol, G.; Hoffmann, R.; Chattergoon, M. A.; Lovas, S.; Cudic, M.; Bulet, P.; Condie, B. A.; Rosengren, K. J.; Montaner, L. J.; Otvos, L. Identification of crucial residues for the antibacterial activity of the proline-rich peptide, pyrrhocoricin. *Eur. J. Biochem.* **2002**, *269*, 4226–4237.
(29) Zhou, X. X.; Li, W. F.; Pan, Y. J. Functional and structural characterization of apidaecin and its N-terminal and C-terminal fragments. *J. Pept. Sci.* **2008**, *14*, 697–707.
(30) Czihal, P.; Hoffmann, R. Mapping of apidaecin regions relevant for antimicrobial activity and bacterial internalization. *Int. J. Pept. Res. Ther.* **2009**, *15*, 157–164.
(31) Mattiuzzo, M.; Bandiera, A.; Gennaro, R.; Benincasa, M.; Pacor, S.; Antcheva, N.; Scocchi, M. Role of the *Escherichia coli* SbmA in the antimicrobial activity of proline-rich peptides. *Mol. Microbiol.* **2007**, *66*, 151–163.
(32) Livermore, D. M. Has the era of untreatable infections arrived? *J. Antimicrob. Chemother.* **2009**, *64*, 29–36.
(33) Liebscher, M.; Roujeinikova, A. Allosteric coupling between the lid and interdomain linker in DnaK revealed by inhibitor binding studies. *J. Bacteriol.* **2009**, *191*, 1456–1462.
(34) Morell, M.; Czihal, P.; Hoffmann, R.; Otvos, L.; Aviles, F. X.; Ventura, S. Monitoring the interference of protein−protein interactions in vivo by bimolecular fluorescence complementation: the DnaK case. *Proteomics* **2008**, *8*, 3433–3442.
(35) Kragol, G.; Lovas, S.; Varadi, G.; Condie, B. A.; Hoffmann, R.; Otvos, L. The antibacterial peptide pyrrhocoricin inhibits the ATPase actions of DnaK and prevents chaperone-assisted protein folding. *Biochemistry* **2001**, *40*, 3016–3026.
(36) Ronald, A. The etiology of urinary tract infection: traditional and emerging pathogens. *Dis. Mon.* **2003**, *49*, 71–82.
(37) Singer, D.; Lehmann, J.; Hanisch, K.; Hartig, W.; Hoffmann, R. Neighbored phosphorylation sites as PHF-tau specific markers in Alzheimer's disease. *Biochem. Biophys. Res. Commun.* **2006**, *346*, 819–828.
(38) Amsterdam, D. Susceptibility Testing of Antimicrobials in Liquid Media. In *Antibiotics in Laboratory Medicine*, 4th ed.; Lorian, V., Ed.; Lippincott Williams & Wilkins: Baltimore, MD, 1996; pp 52−111.
(39) Hoffmann, R.; Vasko, M.; Otvos, L. Serum stability of phosphopeptides. *Anal. Chim. Acta* **1997**, *352*, 319–325.
(40) Yang, S.-T.; Lee, J. Y.; Kim, H.-J.; Eu, Y.-J.; Shin, S. Y.; Hahm, K.-S.; Kim, J. I. Contribution of a central proline in model amphipathic alpha-helical peptides to self-association, interaction with phospholipids, and antimicrobial mode of action. *FEBS J.* **2006**, *273*, 4040–4054.